Vol 17 No 7, July 2008
1674-1056/2008/17(07)/2557-05

Chinese Physics B

© 2008 Chin. Phys. Soc.
and IOP Publishing Ltd

# Design of novel three port optical gates scheme for the integration of large optical cavity electroabsorption modulators and evanescently-coupled photodiodes*

Liao Zai-Yi(廖栽宜)†, Yang Hua(杨 华), and Wang Wei(王 圩)

*State Key Laboratory on Integrated Optoelectronics and Key Laboratory of Semiconductors Materials of Chinese Academy of Sciences, Institute of Semiconductors, Chinese Academy of Sciences, Beijing* 100083, *China*

(Received 21 August 2007; revised manuscript received 7 January 2008)

This paper presents a novel scheme to monolithically integrate an evanescently-coupled uni-travelling carrier photodiode with a planar short multimode waveguide structure and a large optical cavity electroabsorption modulator based on a multimode waveguide structure. By simulation, both electroabsorption modulator and photodiode show excellent optical performances. The device can be fabricated with conventional photolithography, reactive ion etching, and chemical wet etching.

**Keywords:** electro-absorption modulator, uni-carrier photodiode, beam propagation method, monolithic integration

**PACC:** 4280L, 4282

## 1. Introduction

Integrated photodiode (PD) and electroabsorption modulator (EAM) optical gates have become very attractive in optical signal processing lately. The operation is mature and stable because it is an optical–electrical–optical type device and has high speed-operation capacity due to its short electrical interconnecting distance and release of electrical amplification.[1] It has demonstrated a very short open gate time of 2.3ps and has been used in diversiform optical signal processes.[2−5] It suffers from high light power consumption due to low responsivity of the planar PD. By adopting a waveguide type PD, these devices could serve as a transceiver used in 40Gb/s wavelength conversion if integrated with lasers and semiconductor optical amplifiers.[6]

Though the results of these devices are often reported, their fabrication and design details are seldom mentioned. To design PD in these devices, we must not only enhance its responsivity and bandwidth, but also insure that its radio frequency (RF) output is high enough to drive EAM directly. To design EAM, we must reduce its insertion loss and drive voltage. Evanescently coupled waveguide-fed uni-travelling carrier (UTC)-PD is the best choice in PD-EAM optical gate applications because it can simultaneously achieve high output, high responsivity, and high bandwidth.[7−10] It is based on a multimode waveguide structure, while an EAM waveguide must operate in a single-mode. One optional method is integrating single mode spot-size-convertors to reduce insertion loss,[11] but this requires complex fabrication steps, such as sub-micron microlithography and etching. Here we propose a large optical cavity (LOC) structure EAM to integrate a PD, which requires much simpler fabrication techniques and fewer steps.

In this paper, a novel scheme is presented to monolithically integrate evanescently–coupled UTC-PD photodiode with a planar short multimode waveguide structure (PSMW) with LOC-EAM. The three optical ports are in different directions, which make them easy to couple with fibre. The optimized design analysis, the fabrication process, and the results simulated by using the beam propagation method are also presented in detail below.

*Project supported by the National Natural Science Foundation of China (Grant No 90401025) and the National 973 project (Grant No 2006CB604901).

†E-mail: Lzy1348@semi.ac.cn

## 2. Optical design and optimization

Figure 1 is a schematic drawing of the PD-EAM. The signal light is coupled into UTC-PD and converted into an RF signal to drive EAM directly by electrical connection. Waveguide (WG)-PD and EAM are in separate directions, making it possible to adjust each port when aligning fibre with the waveguide. The chip has an area of 0.6mm×0.8mm. The active region of EAM, which employs InGaAsP/InGaAsP multiple-quantum-wells (MQW), is 300 $\mu$m long, and the passive region on each side is 150 $\mu$m long. The input waveguide of the PD is 20 $\mu$m and the absorbed region is $6\mu\text{m}\times 50\mu\text{m}^2$.

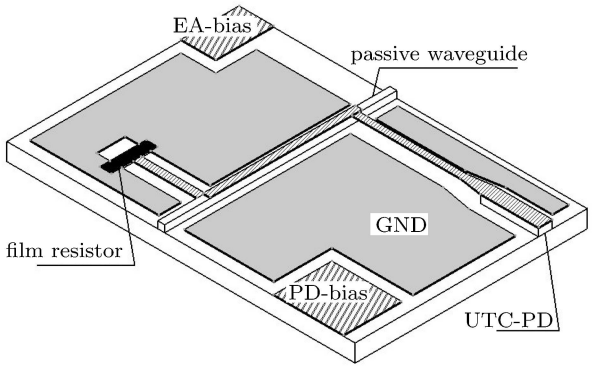



**Fig.1.** Schematic drawing of a PD-EAM optical gate.

### 2.1. PSMW UTC-PD design

A schematic cross section of the PSMW UTC-PD is shown in Fig.2. The multimode waveguide consists of a 1.15Q n-waveguide and two optical matching layers. Different from the PIN structure, the absorber of the UTC structure consists of a 250nm gradually doping P-InGaAs layer. Two optical matching layers are un-doped and serve as a collecting layer. Optical coupling between the fibre and the WGPD is our primary concern. The coupling efficiency $\eta$ is calculated by integration over the area of overlap between the normalized optical field of the light emitted from a single-mode fibre $\varphi(x,y)$ and the normalized optical field of the light guided through the WGPD $\Phi_{i,j}(x,y)$:

$$\eta = \sum_{i,j} \left| \iint \varphi(x,y)\Phi_{i,j}(x,y)\mathrm{d}x\mathrm{d}y \right|^2 ,$$

where $i$ and $j$ are the orders in the horizontal and vertical directions of the guided light mode at the WG-PD, respectively. If the waveguide exists second order mode, the coupling efficiency can increase dramatically, attributable to the higher order modes.[12] Figure 3 shows that the coupling efficiency can reach higher than 80% with a 1.1 $\mu$m 1.15Q lower waveguide, while the efficiency of traditional WG-PD (0.1 $\mu$m lower and upper separate confinement heterojunction (SCH) layer and 0.25 $\mu$m absorption layer) is below 60%.

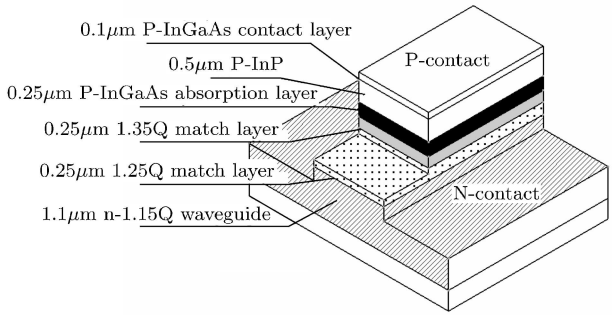



**Fig.2.** Schematic of PSMW-UTC-PD.

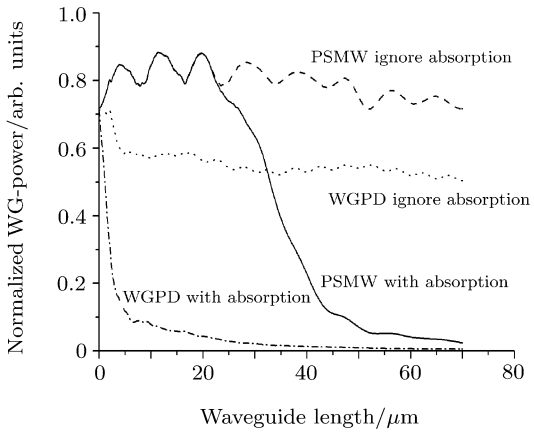



**Fig.3.** Simulated optical power absorption distribution along the waveguide direction for PSMW-PD and traditional WG-PD.

The PSMW structure also improves high-power performance of the PD. In the WGPD, the input light is directly focused on the edge of the InGaAs absorption layer, while, in the PSMW-PD, the input light is focused on the passive guide layer, and gradually penetrates into the absorption layer. Thus, for the PSMW-PD, the photocurrent density in the vicinity of the input edge of the absorption layer is greatly reduced in comparison with that for the WGPD. This reduction implies that the PSMW-PD will be more saturated under higher-input-power conditions than the WGPD. Figure 3 shows that most optical power is absorbed in first 5 $\mu$m in WG-PD, while optical

power is near-linearly absorbed over the 20 $\mu$m region in PSMW-PD.

The thickness of the index matching layer needs to be optimized. If it is too thin, mode beating cannot be obtained and the coupling process is too slow. Consequently, it needs a long absorption distance, which leads to larger capacitance. However, if the index matching layer is too thick, optical power is strongly guided in this layer and mode beating cannot be obtained either. The simulated result is shown in Fig.4. When the index matching layer is inserted, mode beating results, and the optical power in the absorption layer increases. Moreover, the etching of the input guide must be deep enough, otherwise the optical beam is less laterally confined, resulting in losses. The etching depth is set to around 0.5 $\mu$m to ensure fabricated compatibility with EAM.

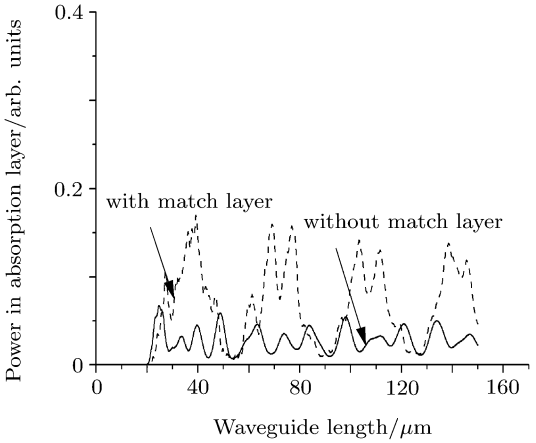



**Fig.4.** Optical intensity in the absorption layer with the match layer and without the match layer.

## 2.2. LOC-EAM design

Figure 5 shows a cross sectional view of the LOC-EAM. A 0.15 $\mu$m 1.25Q index matching layer and a 1.1 $\mu$m 1.15Q lower waveguide layer are inserted under the traditional symmetrical sandwich structure. Coupling efficiency is very important in the EAM design. A large insertion loss will lead to a lower RF-gain and relatively higher noise. Assuming the fibre mode and waveguide mode is a Gaussian distribution, we can represent the coupling efficiency $\eta$ as follows:[13]

$$\eta = \frac{4}{\left(\frac{w_x}{a} + \frac{a}{w_x}\right)\left(\frac{w_y}{a} + \frac{a}{w_y}\right)},$$

where $w_x$ and $w_y$ are the spot size of the waveguide in the horizontal and vertical directions respectively, and $a$ is the spot size of fibre. Coupling efficiency will increase if $w_x$, $w_y$ and $a$ are close to each other. Figure 6 shows that the LOC structure supports a nearly-circular fundamental optical mode similar to that of the lensed fibre, which leads to high coupling efficiency between the waveguide and the lensed fibre.

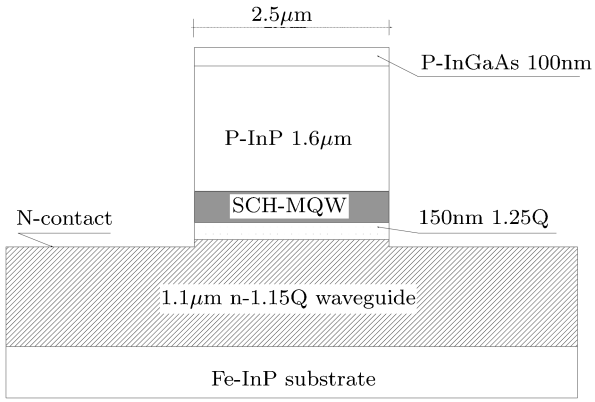



**Fig.5.** Schematic cross section of the LOC-EAM.

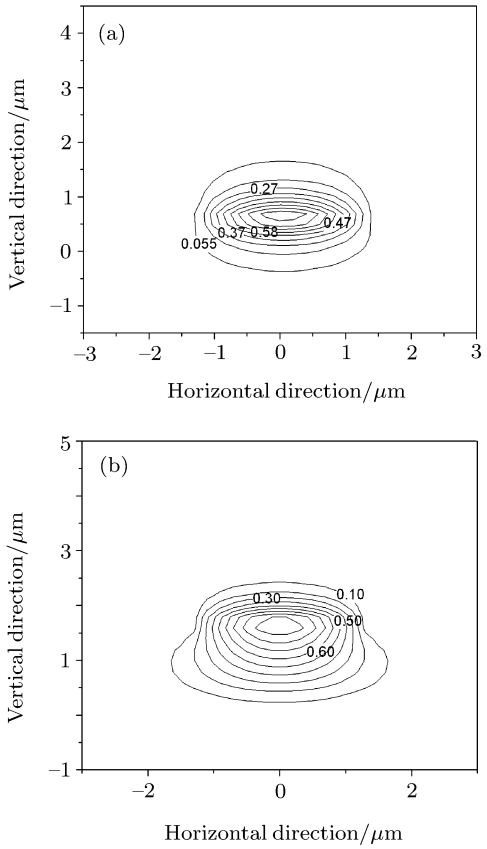



**Fig.6.** Intensity distribution of waveguide modes (a) without lower waveguide layer (b) with lower waveguide layer.

Figure 7 demonstrates that a thicker lower waveguide layer leads to a larger $w_y$, which means that better mode matches with fibre but a lower optical confinement factor reduces modulation efficiency. Furthermore, a thick lower waveguide layer crystal is difficult to epitaxy, so the lower waveguide layer is set

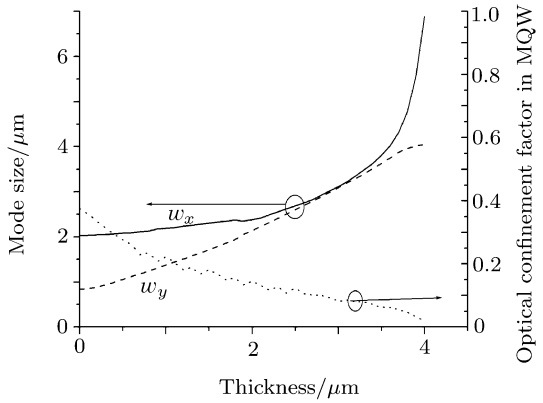



**Fig.7.** Measured near-field spot patterns of EAM (a) without lower waveguide layer (b)with lower waveguide layer.

to 1.1 $\mu$m. After the 1.1 $\mu$m lower waveguide layer is added, by simulation, the mode sizes in the horizontal and vertical directions are expanded to 2.23 $\mu$m×1.45 $\mu$m from 2.02 $\mu$m×0.85 $\mu$m, and the beam divergence angles in the horizontal and vertical directions decrease to 29.5°×40.0° from 36.5°×49.0°, and the optical confinement factor is 0.2. Such a LOC-EAM was fabricated and compared with one without the LOC structure.[14] Figure 8 indicates that the measured near-field spot shape is more circular after the LOC structure is added, and the measured beam divergence angles in the horizontal and vertical directions decrease to 25°×35° from 30°×52°, which is consistent with the simulation results.

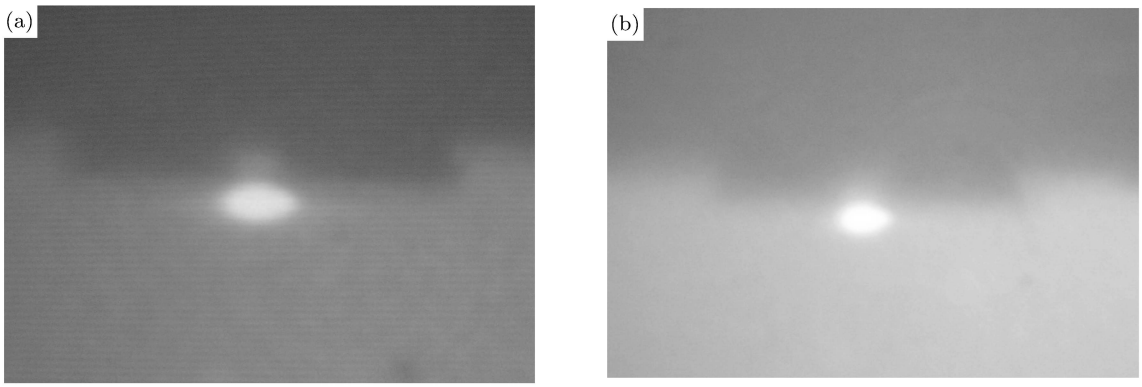



**Fig.8.** Spot-size in the horizontal and vertical direction, and optical confinement factor versus the thickness of the lower waveguide layer.

## 3. Material growth and fabrication

The device can be easily fabricated using a low-pressure metal-organic vapour phase epitaxial process with conventional photolithography. For the first epitaxial growth, an InP buffer, a 1.1 $\mu$m-thick-1.15 lower waveguide layer, a 0.15 $\mu$m 1.25 index-matching layer, a MQW and a SCH stack, and a 150-nm undoped InP implant buffer layer are grown. The passive sections of EAM are then blue-shifted through a P ion implantation quantum well intermixing process. P-InP overcladding, and an InGaAs cap layer are grown in the second epitaxial growth step. A PSMW UTC-PD structure is grown in the third epitaxy after selectively etching the PD region to the index-matching layer with a 250nm SiO2 mask.

In our design, the fabricated processes of PSMW-PD and EAM are compatible, so the fabricated process is the same as that of a single PSMW-PD.[15] It contains self-aligned dry etching, polyimide planarization, airbridge-electroplating, and finally V-groove cleaving, which is reported in Ref.[16] in detail.

## 4. Conclusions

In this paper, a novel method is proposed to integrate LOC-EAM with evanescently coupled waveguide-fed UTC-PD based on a multimode waveguide structure. Both the EAM and PD benefit from the lower multimode waveguide. In simulations, LOC-EAM is released from mode-hopping problem. Its mode size is 2.23 $\mu$m×1.45 $\mu$m, and the beam divergence angles in the horizontal and vertical directions are as small as 29.5°×40.0°. The PSMW-PD shows high coupling efficiency and high power performance ability. It is easy to align into fibre because the three optical ports are in different directions. The crystal epitaxy growth scheme is feasible and the fabrication process is the same as the single PSMW-PD, which make integration easy.

# References


[1] Demir H V, Sabnis V A, Fidaner O, Zheng J F, Harris J S and Miller D A B 2005 *IEEE J. Selected Topic in Quantum Electronics* **11** 86

[2] Kodama S, Yoshimatsu T and Ito H 2004 *Electron. Lett.* **40** 555

[3] Kodama S, Yoshimatsu T and Ito H 2004 *Electron. Lett.* **40** 626

[4] Kodama S, Yoshimatsu T and Ito H 2004 *Electron. Lett.* **40** 696

[5] Kodama S, Yoshimatsu T and Ito H 2005 *IEEE Photon. Technol. Lett.* **17** 2367

[6] Raring J W and Coldren L A 2007 *IEEE J. Selected Topics in Quantum Electronics* **13** 3

[7] Jasmin S, Vodjdani N, Renaud J C and Enard A 1997 *IEEE Trans. Microwave Theory and Techniques* **45** 1337

[8] Takeuchi T, Nakata T, Makita K and Yamaguchi M 2000 *Electron. Lett.* **36** 972

[9] Li N, Demiguel S, Chen H, Zhang X, Campbell J C, Wei J, Lu H and Anselm A 2005 *Optical Fiber Communication Conference* **1** 3

[10] Shi J W, Wu Y S, Wu C Y, Chiu P H and Hong C C 2005 *IEEE Photon. Technol. Lett.* **17** 1929

[11] Young-Shik Kang, Sung-Bock Kim, Yong-Duck Chung and Jeha Kim 2005 *Laser and Electro-Optics Society* 422

[12] Kato K, Hata S, Kawano K, Yoshida, J and Kozen A 1992 *IEEE J. Quantum Electronics* **28** 2728

[13] Wang S Y and Lin S H 1988 *J. Lightwave Technol* **6** 758

[14] Yang H 2007 *Acta Phys. Sin.* **56** 2751 (in Chinese)

[15] Magnin N, Harari J, Marceaux J, Parillaud O, Decoster D and Vodjdani N 2006 *IEE Proc-Optoelectron.* **153** 199

[16] Li N, Demiguel S, Chen H, Zhang X, Campbell J C, Wei J, Lu H and Anselm A 2005 *Optical Communication Fiber Conference* **1** 3